Heliyon 7 (2021) e06017

Contents lists available at ScienceDirect

Heliyon

journal homepage: www.cell.com/heliyon

Research article

Verification of Gardner's equation and derivation of an empirical equation for anhydrite rocks in Sirte basin, Libya: case study

Bahia M. Ben Ghawar [a,*], Moncef Zairi [b], Samir Bouaziz [c]

[a] Département De Génie Géoressources Et Environnement, National School of Engineers of Sfax, Tunisia
[b] Department of Civil Engineering, National School of Engineers of Sfax, Tunisia
[c] Geology Department, National School of Engineers of Sfax, University of Sfax, Tunisia

ARTICLE INFO

Keywords:
Bulk density
Anhydrite rocks
Gardner's equation
Travel time
Sirte basin
Libya

ABSTRACT

Bulk density is a physical property of rocks measured in the laboratory on rock samples or obtained from oil field logging tools. When bulk density is not measured, a synthetic bulk density log can be calculated, for which Gardner's equation is the most widely used. However, Gardner's equation might not be appropriate for regions in which the density–velocity relationship does not conform to Gardner's curves. Here, we verified the applicability of Gardner's equation to calculation of synthetic bulk density of anhydrite rocks in the Sirte Basin (Libya) and compared the results to those obtained from an equation derived from the available measured bulk density and sonic logs. We used fifteen wells to calibrate Gardner's equation and three wells to derive an equation for the anhydrite rocks. The anhydrite rocks were 10–510 feet thick. The bulk density calculated by Gardner's equation differed only slightly from the measured log values, with the exception of the eastern part of the Sirte Basin. The average of the differences in bulk density between the measured values and Gardner's equation results were 0.022–0.040 g/cm^3, and between the measured values and the derived equation results 0.002–0.045 g/cm^3, both with a standard error of about 0.01 of the bulk density estimated results. We conclude that while Gardner's equation is more appropriate for estimating the bulk density of anhydrite rocks in the eastern part of the basin, the derived equation could be more appropriate for the western region.

1. Introduction

Determination of the bulk density (ρ_b) in oil fields is the starting point for seismic survey, petrophysical evaluation, mechanical properties evaluation and stress analysis. The relationships between ρ_b and other rock properties have been widely investigated. Mavko et al. (2009) summarized the relation between bulk density and P-wave velocity of different rock types. In well logging data, anhydrite rocks are characterized by high ρ_b and low primary velocity (Vp). Gardner et al. (1974) demonstrated a simple systematic relationship between seismic P-wave velocity ($Vp = 1/\Delta T$) and density (ρ) of different types of sedimentary rocks. To evaluate the distribution of anhydrite rocks in the San Andres reservoir, USA, Pranter et al. (2004) worked on the core samples and seismic data of the wire lines from 120 wells by using cross-plots of apparent matrix grain density *versus* apparent matrix volumetric cross-section (ρ_{maa}–U_{maa}) combined with Vp/Vs seismic attributes. Dey and Stewart (1997) concluded that Gardner's relationship seems to give a poorer estimation of the Gardner exponent than the use of shear wave velocity (Vs). Moreover, Rafavich et al. (1984) concluded that Gardner's equation underestimates the density of anhydrite rocks. More recently, Nwozor et al. (2017) derived lithology-specific coefficients of density–velocity in the Niger Delta basin and found that they differed from those derived by Gardner's equation. Clearly, Gardner's equation cannot be considered the default equation for all settings.

Very thick anhydrite rock sequences are typical in the western Sirte basin subsurface but are less common as interlayering beds in the eastern part of the basin and they are absent in its central region. The measured bulk density log is recorded mainly at interesting reservoir depths and are unavailable for other drilled formations. In addition, well logging tools and their values are affected by borehole stability problems, which results from the use of drilling fluids and bit types that are unsuitable for salt formations such as the Gir Formation. Hence, synthetic bulk density calculated by general equations might not give correct estimates because the deposition environment and the structure setting of the sedimentary basin vary from one geographic region to another. Therefore, as Gardner et al. (1974) recommended, in the absence of relevant relationships

* Corresponding author.
E-mail address: gloriamuftah@yahoo.com (B.M. Ben Ghawar).

https://doi.org/10.1016/j.heliyon.2021.e06017
Received 2 January 2019; Received in revised form 16 August 2019; Accepted 13 January 2021

between different specific parameters, we must resort to empirical correlations based on field data. Furthermore, obtaining accurate local results from general equations used worldwide requires calibration. To that end, we examined the applicability of Gardner's equation for estimation of bulk density of anhydrite rocks in Sirte basin, Libya, and simulated Gardner's procedure based on ρ and Vp to derive an empirical equation from the well log data of 17 wells in different parts of that basin.

2. Geologic setting

Sirte basin is one of the largest sources of hydrocarbons in Libya. It is bounded on the north by the Gulf of Sirte, on the northeast by Cyrenaica Platform, on the southeast by Jabal Al Dalmah Arch, on the south by Tibesti Massif, on the southwest by Murzuq Basin, and on the west by the Ghadames Basin. Structurally, tectonic subsidence studies of the Sirte Basin (Gumati and Nairn, 1991) indicate that a relatively slow rate of subsidence from Cenomanian to Maastrichtian stage, and more rapid and a uniform rate of subsidence during the period from Maastrichtian to mid Eocene. The dominant structural features of the Sirte Basin are series of northwest-southeast striking horst and graben structures (Figure 1), which developed in response to Late Cretaceous to Eocene rifting. The Hun Graben and Ajdabiya Trough subsided with different rates up to 500 m. In Miocene time, most of the Sirte basin was tilted toward the northeast and a great thickness of sediments has accumulated in Ajdabiya Trough, while gentle folding occurred in the southern Sirte basin (Hallett and Clark-Lowes, 2017).

The stratigraphics of Sirte basin can be divided into the following megasequences: pre-rift (Precambrian–Ordovician?), syn-rift (l. Jurassic–Eocene) and post-rift (Oligocene–recent) (Gras, 1996). The sedimentary sequence may have changed in thickness over time (Figure 2), depending on the tectono-stratigraphic setting in different parts of the basin (El-Hawat, 1992). Therefore, the main reservoirs range in age from fractured Precambrian basement to Gargaf Sandstone (Cambrian–Ordovician), Nubian Sandstone (Lower Cretaceous), Bahi Sandstone (Upper Cretaceous), Upper Satal, Beda, Dahra and Zaltan (Palaeocene). In addition, carbonates in shoals and Bioherm (Eocene) are also form reservoir rocks.

Abdunaser (2015) reviewed petroleum geochemical evaluation in the western Sirte Basin based on published studies and unpublished companies' reports. More interesting are the studies by Robertson Group

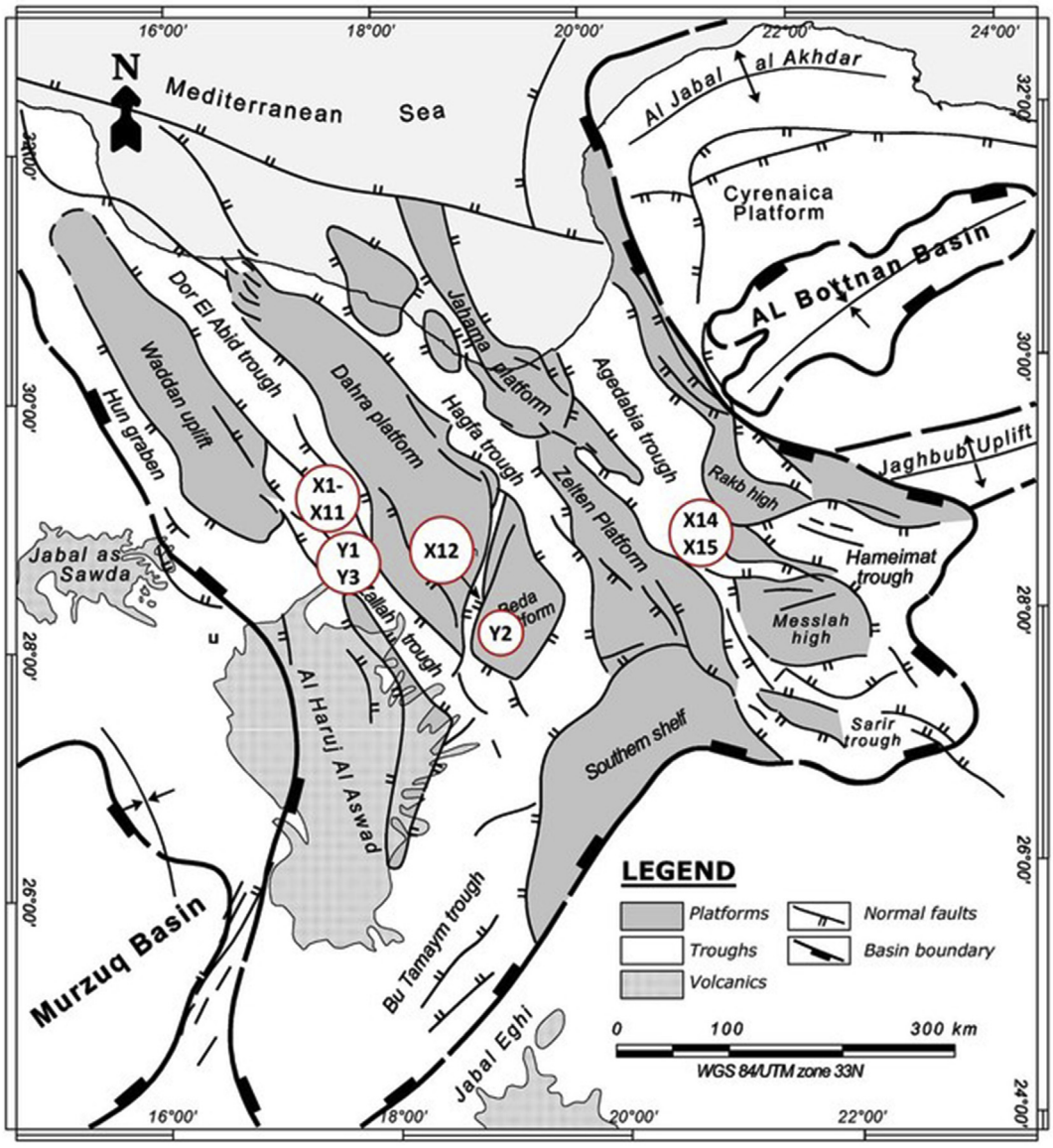

Figure 1. Major structural elements of Sirte Basin (after (Musbah Abadi, 2002). Red circles are well-sampling locations and the numbers within refer to the well numbers.

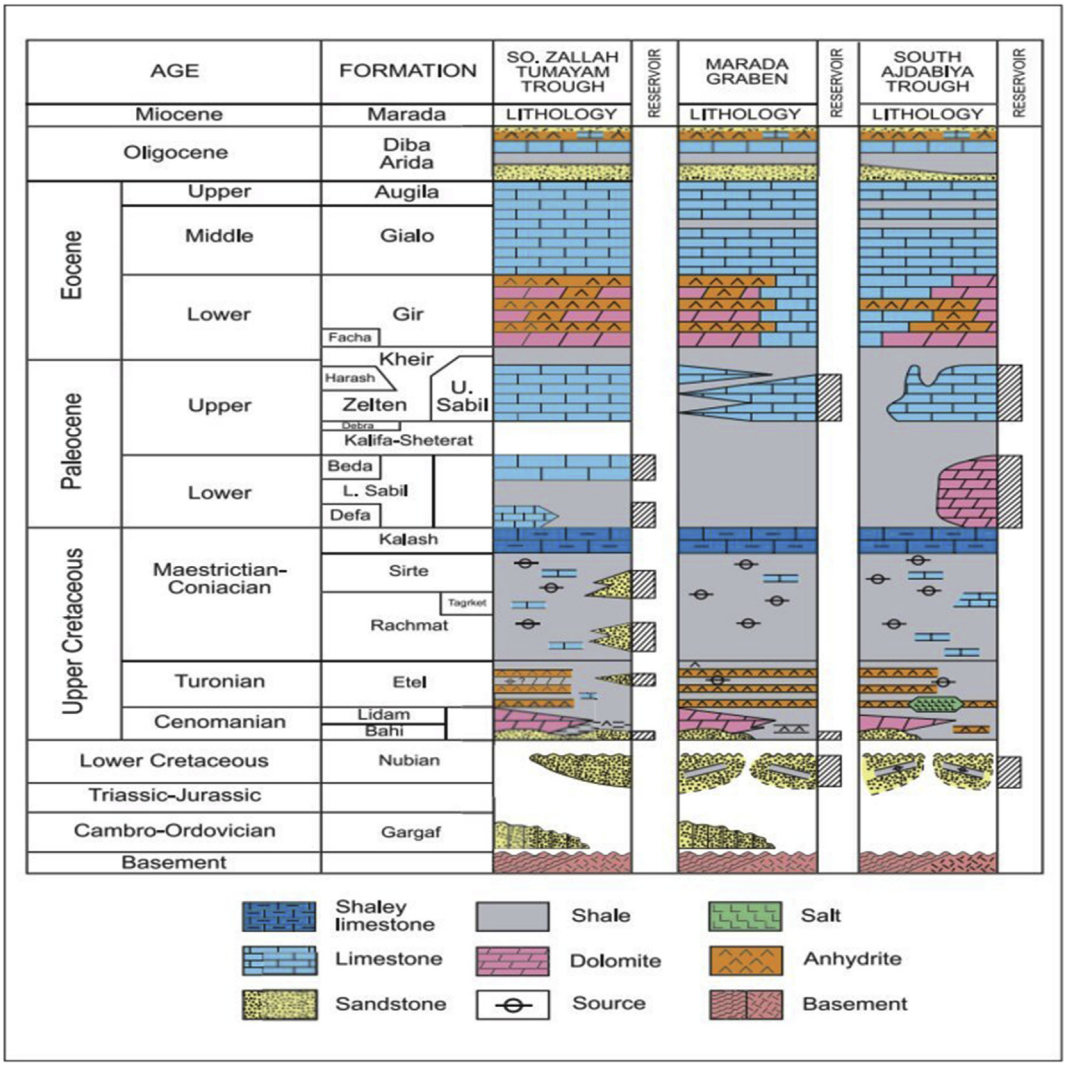

Figure 2. Generalized stratigraphic correlation chart of the Sirte basin (Rusk, 2001).

(1989) and El-Alami et al. (1989), who described the Sirte (Rakb) shale and Rachmat Formations of the Upper Cretaceous age as the principal source rocks in the Western Sirte Basin. Robertson Group concluded that both source rocks contain mixed-type Kerogen and degraded humic material in grabens depocenters. The Upper Cretaceous Sirte Shale unit consists of amorphous rock with a minor amount of algal herbaceous material in both the Zallah and Maradah Troughs. The total organic carbon (TOC) ranged from 1.9% to 3.8% in the Zallah Trough.

Sirte shale Formation (Upper Cretaceous) has been reported to be the source rock of the hydrocarbon resources in Sirte Basin, but it is not the source rock in the western part (Hun Graben) (Ambrose, 2000; El-Alami, 1996; Ghori and Mohammed, 1996; Gumati and Schamel, 1988; Macgregor and Moody, 1998; Mansour and Magairhy, 1996; Montgomery, 1994) Hence, Sirte Shale is the only main mature source rock in the northern Zallah Trough and Dur al Abd Trough (Abdunaser, 2015).

El-Alami et al. (1989) explained categorically that there are no other sources, as such as Devonian or Silurian (Basal Tanzuft), in the western part of the Sirte basin. Also, Roohi (1996) attributes the peak oil generation in the Late Eocene– Oligocene period and the time of migration in the Late Oligocene–Miocene period to the subsidence and tilting of the basin during Mid-Eocene. Mid-Triassic lacustrine shales and variegated shales (Mid-Cretaceous) are other source rocks detected in the eastern part of the Sirte basin. Two different crude oil families have been discovered in Intisar fields, which have the same organic matter type, lithology, maturity and geologic age but had migrated from different pathways, indicating the presence of at least two different source rocks deposited in redox environment in the eastern part of Sirte Bain (Faraj et al., 2016).

Hun Evaporite is one of the major thick members of the Gir Formation (Lower Eocene), which reaches a thickness of about 600 m in the Zallah Trough (Abdunaser, 2015). It is composed primarily of anhydrite, smaller amounts of polyhalite, and minor amounts of dolomite and clay, which serves as a cap rock of the major western Facha Member reservoir. During the Eocene epoch, the Zallah trough was characterized by a down-warping phase, which in turn witnessed a special event that might indicate that the rate of primary sedimentation was higher than the rate of decompacted subsidence. Therefore, facies of shallow environment or sea withdrawal are present. For that reason, the Facha Member represents a restricted shelf facies around the margin of the Sirte Basin (El-Bakush et al., 2010). Both the Facha and Hun Members reappear on the Amal Platform in the eastern part of the basin (Figure 3). On the basis of stratigraphic positioning in several of the trough areas (Figure 2), Etal Formation in the eastern part of Sirte basin is composed of thin-bedded dolomites, anhydrites and shales, and the anhydrite rocks provide a very effective seal of Lidam carbonates (Hallett and Clark-Lowes, 2017). Furthermore, interlayering strips of anhydrite are present in some carbonate formations, for instance in the lower part of Sabil and Beda Formations.

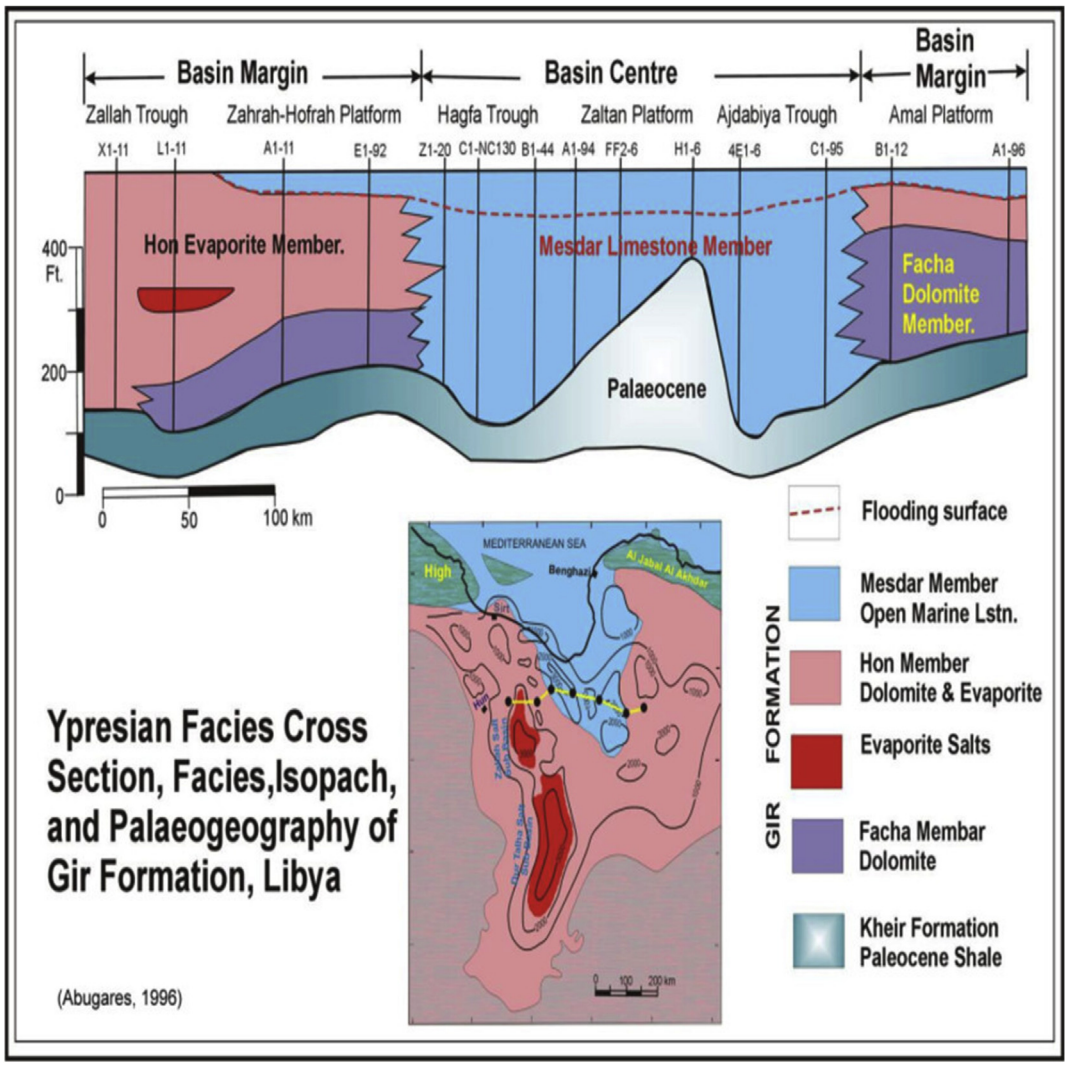

Figure 3. Lower Eocene palaeogeographic map and facies distribution across the Sirte Basin (El Hawat and Pawellek, 2004).

The region covered by this study consists of Zallah Trough, Beda Platform, south Dahra–Hofra Platform and Jalu area in the Sirte Basin (Figure 1). The thickness of the anhydrite beds over the area covered by this study ranges from 10 feet (3.0 m) to 510 feet (155.4 m). These deposited sequences are located at depths in the range of 1300–11000 feet (~396–3352.8 m).

3. Methodology

Anhydrite rocks can be easily identified on logs by certain characteristics and values on wire lines. They have high ρ_b (close to 3 g/cm^3), zero or negative neutron porosity (Øn), high resistivity (R) of up to 2000 ohm m, and stable reading of compressional travel time (ΔTc). The basic physical and engineering properties of anhydrite rocks in the studied region (Schlumberger, 2009) are as follows: ρb log value 2.98 g/cm^3, Øn ~ 0.7% to – 2%, ΔTc ~50 μs/ft, photoelectrical factor (PEF) ~ 5.1 b/e; resistivity >100 Ohm.m, unconfined compressive strength ~97.5 MPa, and Young's modulus (E) ~ 63.9 GPa.

We selected the 17 wells in the region (Figure 1) that contain anhydrite rock and have the main logs (particularly bulk density, and sonic logs). As a representative example, Figure 4 shows these logs for well Y1 in the western Sirte Basin (Zallah Trough), and the anhydrite section above the dashed line (~4280 feet). However, the importance of the bulk density to petrophysical evaluation and construction of a mechanical earth model led us to estimate the bulk density in wells containing anhydrite beds. The data from 15 wells (X1–X14) were used to calibrate Gardner's equation and those from the other 3 wells (Y1–Y3) to derive an empirical equation for the anhydrite rocks.

Generally, the ρb log of a rock is a function of its mineral composition, porosity, water saturation and hydrocarbon fluid type. According to that, conventional incompatible and compatible cross-plotting could be constructed between ρb and other rock properties. One such property is density-neutron cross-plot, which is used as an indicator of anhydrite and the presence of gas. Regions in which neutron porosity is very low and bulk density is high are referred to as anhydrite rock intervals. Cross-plots of bulk density *versus* travel time and travel time *versus* neutron porosity are also used to define evaporite minerals. Figure 5 displays the bulk density–travel time cross-plot of well Y1. Based on the plots constructed for all the wells, the main minerals in the anhydrite beds examined are anhydrite, Langbeinite and polyhalite.

Density and travel time logs represent the porosity indicator of rocks. The ρ_b and Δt logs are linearly related to porosity (Eqs. (1) and (2)). A unit volume of porous rock consists of a fraction made up of pores (Ø) and a fraction (1 − Ø) made up of solid rock matrix. Therefore, the ρ_b of a sample can be written as Eq. (1).

$$\rho_b = \varphi\, \rho_f + (1 - \varphi)\, \rho_{ma} \tag{1}$$

where ϕ is porosity (fraction), ρ_f is density of fluid in the borehole type (g/cm^3), and ρ_{ma} is matrix density (g/cm^3).

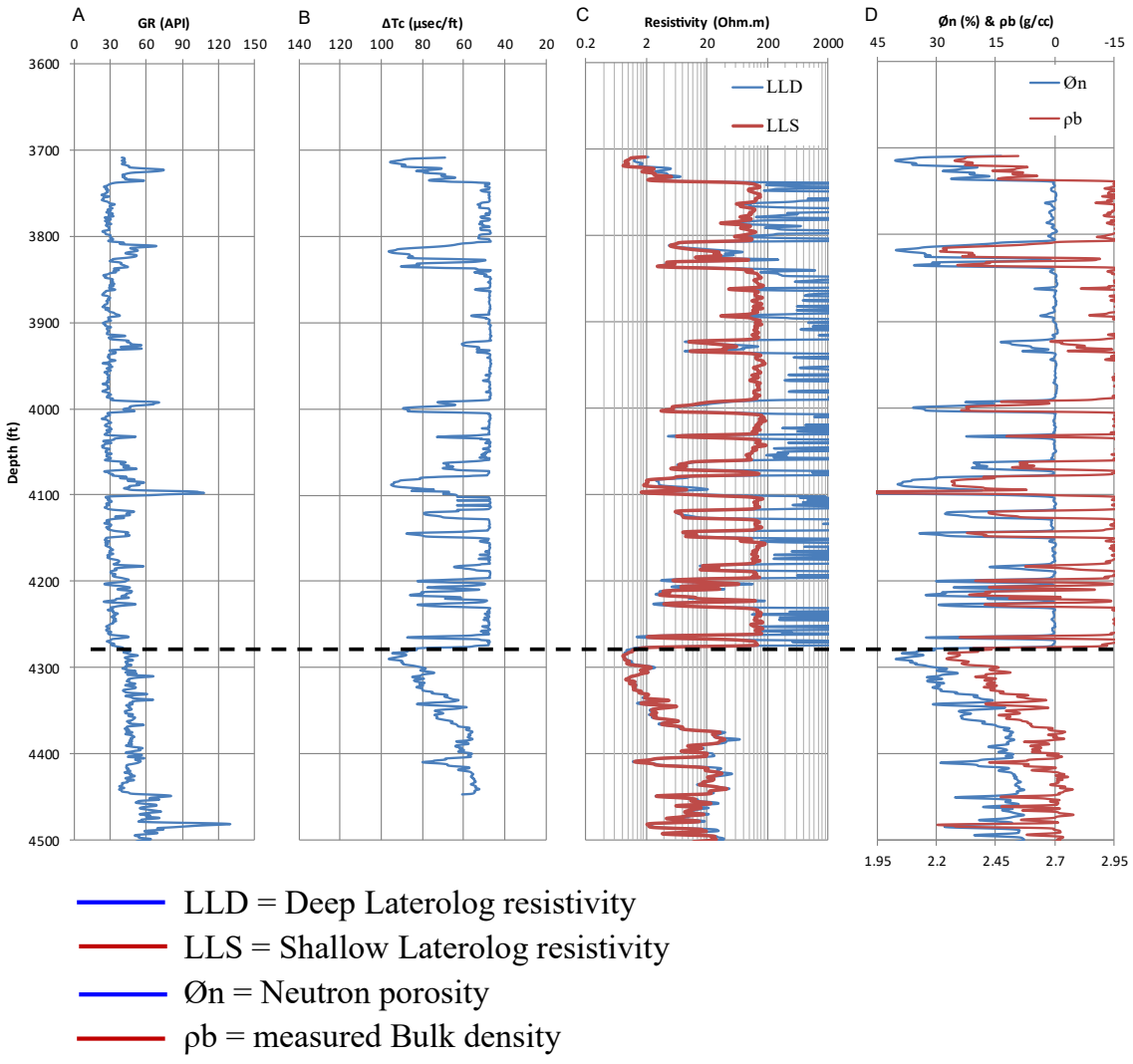

Figure 4. Main logs of well Y1 (Zallah trough). (A) Gamma ray log; (B) compressional travel time (ΔTc); (C) Deep Laterolog (blue: LLD) and shallow Laterolog (red: LLS) resistivity; (D) Neutron porosity (Blue: Øn) and bulk density (red: ρb).

Waveform recording considerably extends the range of sonic logging applications in both open and cased holes (Bateman, 2012). The principal waves recorded by the sonic tools as a received signal are compressional, shear, and fluid waves, as well as guided waves consisting of pseudo-Rayleigh and Stoneley waves (Cheng and Toksoz, 1980). The physical nature of each of these waves has been described by Frei (1983). The basis for the method used to determine formation porosity from sonic logs is that compressional waves travel faster through a solid than through a fluid. The measured Δt and Ø are related (Wyllie time-average; equation 2). All of the wells drilled in Sirte basin have records of the compressional (primary) waves, which were among the raw data used in this work.

$$\Delta t_c = \varphi\, \Delta t_f + (1 - \varphi)\Delta t_{ma} \quad (2)$$

where Δt_c is transit time (μs/ft), Δt_f is fluid transit time in the borehole (μs/ft), and Δt_{ma} is matrix travel time (μs/ft).

4. Calibration of Gardner's equation

Gardner et al. (1974) suggested polynomial and power relations between P-wave velocity and ρ_b for many rock types. Most sedimentary

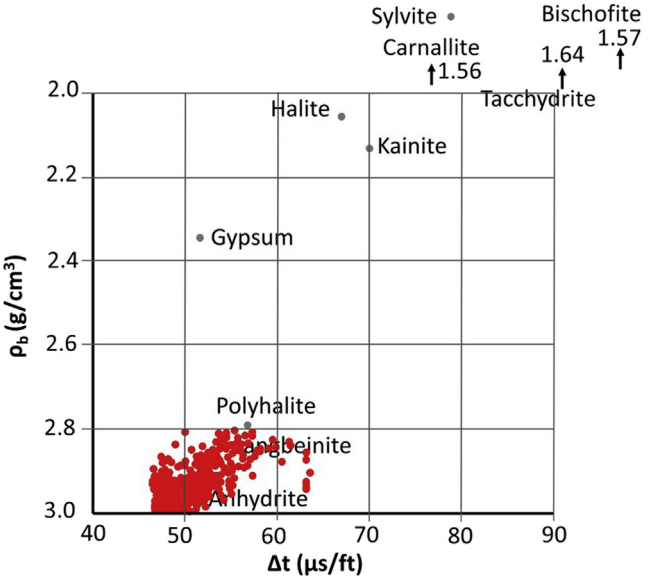

Figure 5. Cross-plot of bulk density *versus* travel time for identification of evaporite minerals in well Y1in Zallah Trough (after Serra (2008)).

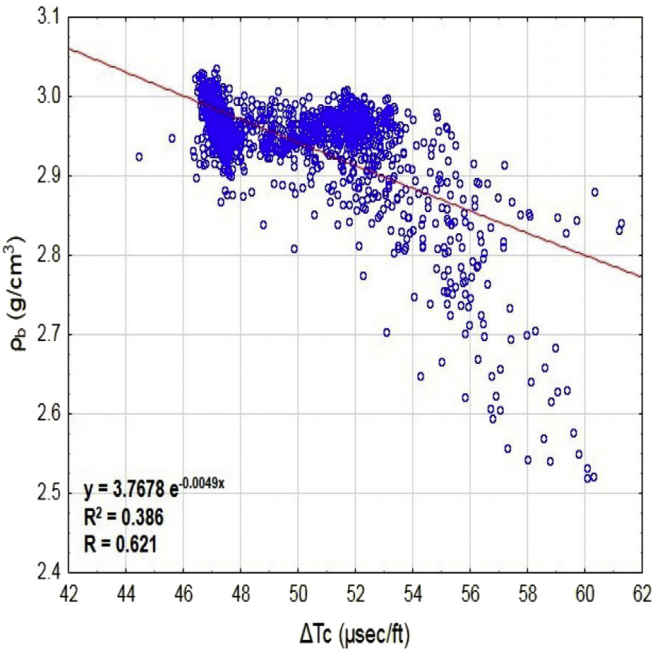

Figure 6. Bulk density (ρb) versus compressional travel time (ΔTc) of anhydrite rocks in we stern Sirte basin, Libya (wells Y1– Y3).

rocks have the same type of this relationship, except anhydrite, coal and salt, which have elasticity behavior different from that of other sedimentary rocks. Also, Rafavich et al. (1984) expressed a relationship between acoustic properties and the petrographic character of carbonate rocks and concluded that velocity is directly related to ρ_b and inversely related to porosity. Krasovsky (1981) showed that Gardner's equation is not universal because in datasets from many sedimentary basins across the world there are several cases where the density–velocity data do not conform to the original Gardner curve. More recently (Nwozor et al. (2017)), showed that Gardner's relation does not appear to give good estimates of density from velocity data of shales and sands in the Niger Delta, which deviate from the general rule. Thus, Eqs. (3) and (4) are different forms of Gardner's empirical equations for anhydrite rocks. Eq. (4) is used to estimate synthetic ρ_b of anhydrite sections within the 17 wells we examined. Hence, the synthetic log results were calibrated with the real measured logs.

$$\rho_b = -\ 0.0203\ V_p^2 + 0.321\ V_p + 1.732 \tag{3}$$

$$\rho_b = 2.19\ V_p^{0.16} \tag{4}$$

where ρ_b is bulk density (g/cm^3) and V_p = compressional wave velocity (km/s) or 1/ΔTc (μs/ft).

5. Derivation of an empirical equation for anhydrite rocks

As mentioned above, the wave velocity is directly related to the density of rocks. Therefore, following Gardner, we empirically derived an equation for the relation between the measured ΔTc and ρb in the logs of three wells (Y1–Y3) for the anhydrite rocks in the Sirte Basin area. It is noteworthy that these wells were selected from three different oil fields in the Zallah trough. The anhydrite sections are associated with the dolomite and salt interlayering beds (Figures 4, 7, and 8). These interlayering parts are delineated by the bulk density–travel time and bulk density–neutron overlay plots. So, the log readings of these interlayering rocks were eliminated to get only the log values of anhydrite rocks.

A scatter-plot of ρ_b *versus* ΔTc was constructed using Statistica Academic software version 13.3 (TIBCO, Statistica), and an empirical equation was fitted by regression analysis.

6. Results and discussion

Figure 6 shows a plot of the measured bulk density and travel time log data of the anhydrite rocks from the three wells. The fitted regression line provides Eq. (5). The appearance of points with bulk density <2.8 g/cm^3 was attributed to the effect of associated minerals (Langbeinite and Polyhalite) and a smaller quantity of dolomite.

$$\rho_b = 3.7678\ e^{-0.0049\ \Delta Tc} \tag{5}$$

To examine the applicability of Gardner's equation and derived empirical equation of the bulk density of the anhydrite rock, four wells in the Sirte Basin were chosen. Table 1 displays a selected part of travel time, neutron porosity and measured bulk density from the well logging data, and the results of both Eqs. (4) and (5) through the anhydrite depth of well X10.

In general, the bulk density results obtained from Gardner's equation and from the derived equations are very close to those in the measured log (Figures 7 and 8).

A gap between the measured and calculated bulk densities in well Y2 (Figure 7, C) at three depth intervals (5020–5030, 5070–5075 and 5145–5150 feet) were attributed to salt interlayering. Figure 8 shows

Table 1. Selected parts of anhydrite interval data and results of well X10.

Depth (ft)	ΔTc (μsec/ft)	$Ø_n$ (%)	ρb measured (g/cm^3)	ρb (g/cm^3) derived equation	ρb (g/cm^3) Gardner et al. (1974)
5511	54.5345	-0.4441	2.774	2.88427	2.88416
5511.5	54.2847	-0.427	2.8244	2.88780	2.88628
5512	54.035	-0.4098	2.8748	2.89134	2.88841
5512.5	53.5355	-0.3989	2.9117	2.89842	2.89270
5513	52.2867	-0.4897	2.9258	2.91621	2.90365
5513.5	52.037	-0.5889	2.9139	2.91978	2.90587
5514	51.5375	-0.688	2.9074	2.92694	2.91036
5514.5	50.7882	-0.7872	2.9796	2.93771	2.91719
5515	51.2378	-0.8863	2.9871	2.93124	2.91308
5515.5	50.2388	-0.9855	2.9793	2.94563	2.92227
5516	49.7892	-1.0306	3.0115	2.95212	2.92648
5516.5	50.4885	-1.0167	3.0258	2.94202	2.91995
5517	50.2887	-1.0029	3.0297	2.94491	2.92181
5517.5	50.5385	-0.9891	3.0006	2.94130	2.91949
5518	50.988	-0.9752	2.9788	2.93483	2.91536

multi-anhydrite strips within Etal Formation at a depth below 11,370 feet in well X14 (Jalu area) in the eastern part of Sirte basin.

The average difference between the computed and the measured bulk densities was calculated for wells X10, X12, Y2, and X14 (Table 2). The average differences were lower for the derived equation than for Gardner's results (0.002–0.045 g/cm^3) than for Gardner's equation (0.022–0.04 g/cm^3) for wells X10, X12, Y2. The exception was well X14. These data reveal that the derived equation has a lower average difference than the Gardner's equation. Reason of difference between the measured and the calculated bulk density by the derived equation in the eastern part of the Sirte Basin in the wells (X13 and X14) is not very clear. It could be related to insufficient of the studied wells numbers in this part. Also, the studied depths (below 11390 feet) of these wells are mainly dolomites with very thin steaks of Anhydrite may cause this high estimated of the bulk density.

The average values of the standard errors (SE) of the estimated bulk density were also calculated, by using Eq. (6) (Table 3).

$$SE = \sqrt{\frac{(\rho_{b\ \text{calculated}} - \rho_{b\ \text{measure}})^2}{n - 2}} \quad (6)$$

where $\rho_{b\ \text{measured}}$ = measured bulk density (g/cm^3), $\rho_{b\ \text{calculated}}$ = calculated bulk densities by the derived and Gardner's equations (g/cm^3), and n = number of observed depths.

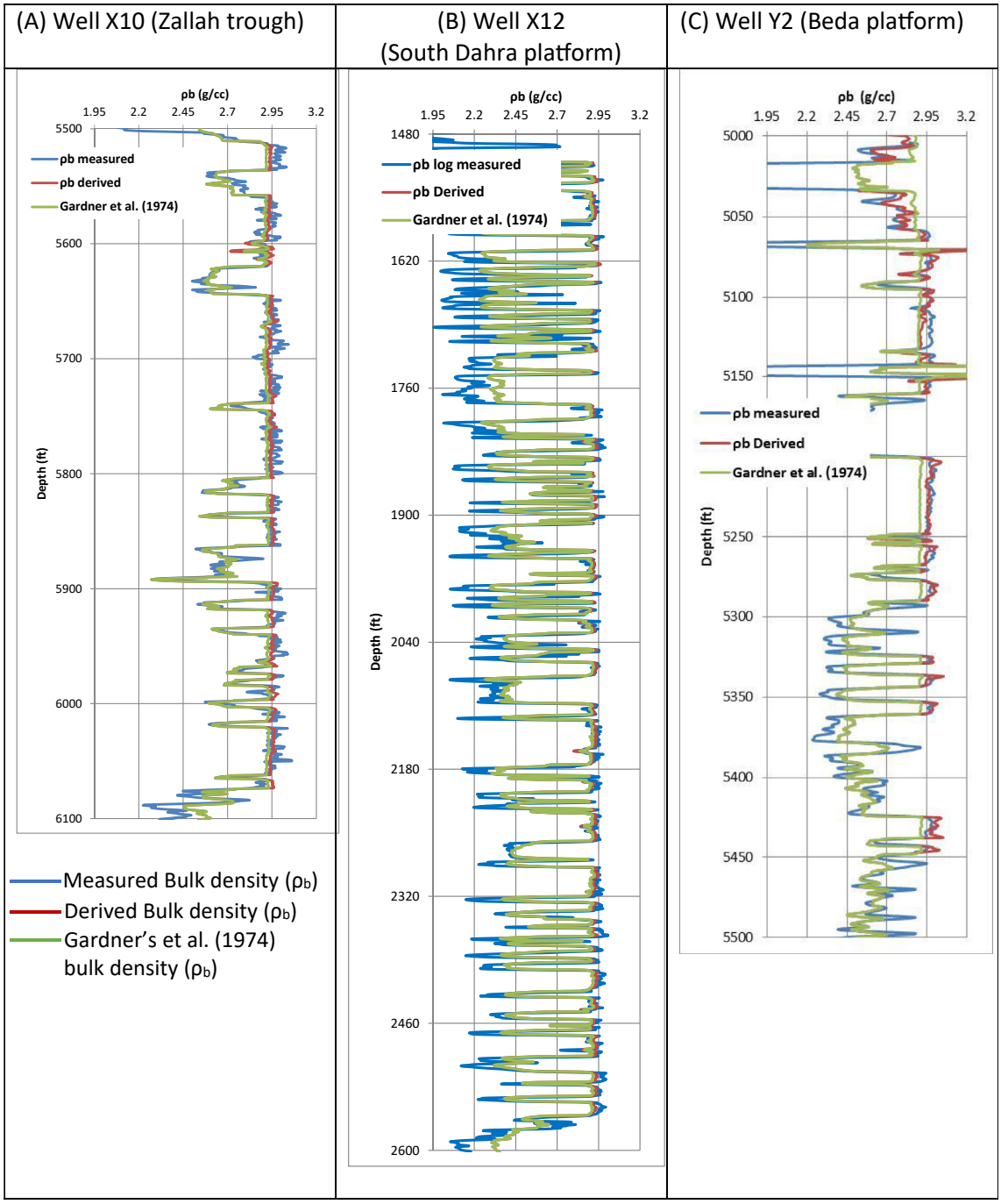

Figure 7. Measured bulk density of three wells compared to bulk density calculated by Gardner's equation and by a derived equation of different wells at different structures, Sirte Basin - Libya. (A) Well X10 Zallah trough; (B) Well X12 South Dahra platform; (C) Well Y2 (Beda platform).

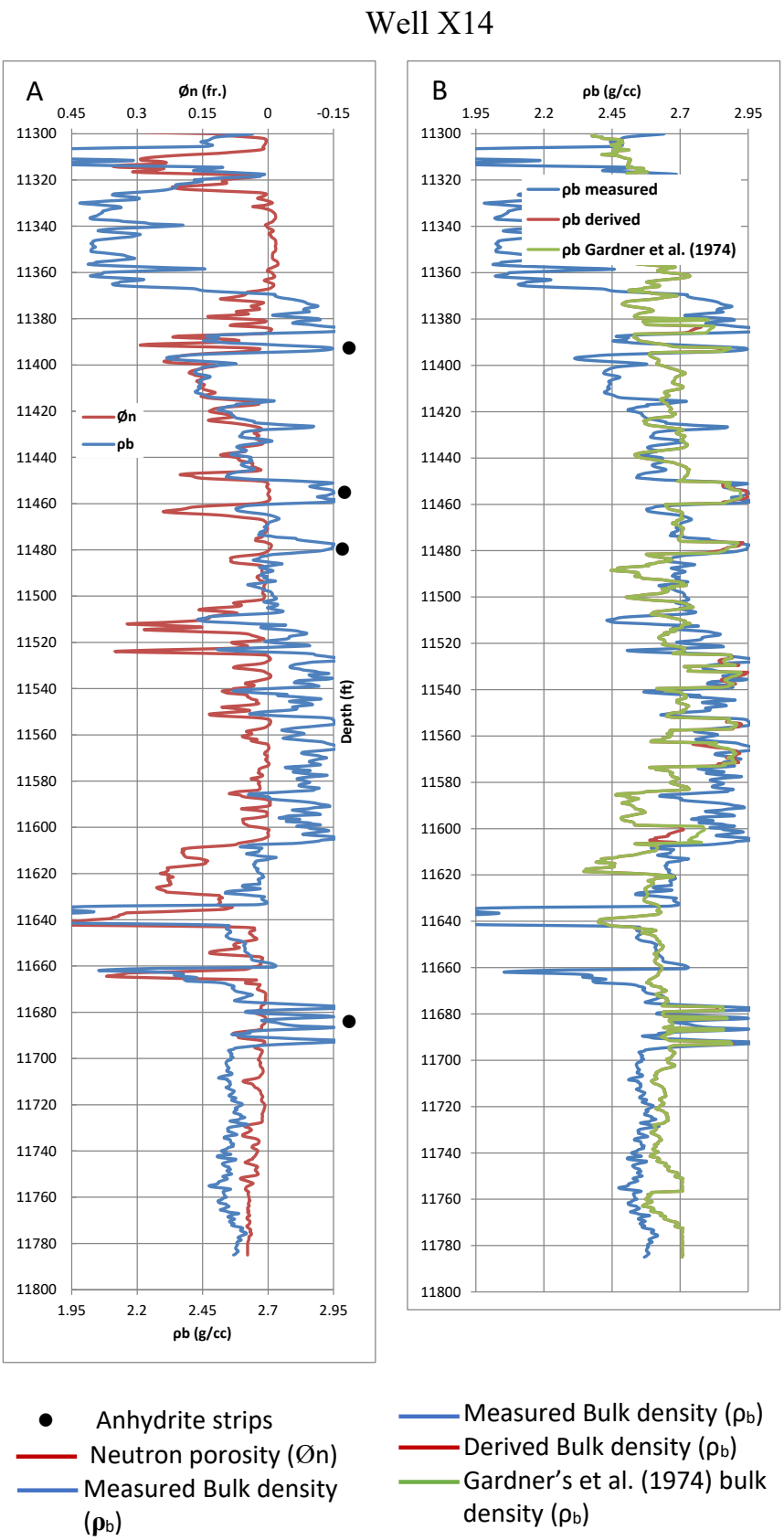

Figure 8. Well X14 (Jalu area). (A) Measured neutron porosity (red: Øn) and bulk density (blue: ρb). (B) Measured bulk density (blue: ρb), derived bulk density (red: ρb) and Gardner et al. (1974) bulk density (green: ρb).

Table 2. Average difference between measured and calculated bulk density.

Well	Measured –derived (g/cm^3)	Measured –Gardner's (g/cm^3)
X10	0.002	0.023
X12	0.009	0.022
Y2	0.013	0.022
X14	0.045	0.040

Table 3. Standard error of the bulk density estimation.

Well	Measured–derived equation (g/cm^3)	Measured–Gardner 's Equation (g/cm^3)
X10	0.045	0.050
X12	0.040	0.044
Y2	0.077	0.087
X14	0.087	0.070

The results obtained from Gardner's equation have smaller standard errors than the derived equation only in wells X13 and X14, in the eastern part of Sirte basin. Based on these results, Gardner's equation seems to be more appropriate in caution for the eastern region of Sirte Basin and encourages using the derived equation in the western part.

7. Conclusion

Based on cross-plots of travel time and bulk density, the main minerals in the studied anhydrite beds in the Sirte Basin are anhydrite, Langbeinite, and Polyhalite. Though Gardner's equation is unsuitable for some regions in the world, it is appropriate for the eastern part of the Sirte basin in caution because an insufficient number of wells have been studied in that part of basin, but our derived equation is more appropriate for the western Sirte basin.

Declarations

Author contribution statement

B. M. B. Ghawar: Conceived and designed the analysis; Performed the experiments; Analyzed and interpreted the data; Contributed analysis tools or data; Wrote the paper.

M. Zairi, S. Bouaziz: Analyzed and interpreted the data; Contributed analysis tools or data; Wrote the paper.

Funding statement

This research did not receive any specific grant from funding agencies in the public, commercial, or not-for-profit sectors.

Competing interest statement

The authors declare no conflict of interest.

Additional information

No additional information is available for this paper.

Acknowledgements

We thank the National Oil Corporation in Libya (NOC) and all its oil companies for providing only the data used in this study.

References

Abdunaser, K., 2015. Review of the petroleum geology of the western part of the Sirt Basin, Libya. J. Afr. Earth Sci. 111, 76–91.
Ambrose, G., 2000. The geology and hydrocarbon habitat of the sarir Sandstone, SE sirt basin, Libya. J. Petrol. Geol. 23 (2), 165–192.
Bateman, R.M., 2012. Openhole Log Analysis and Formation Evaluation, second ed. Society of Petroleum Engineers.
Cheng, C.H., Toksoz, M.N., 1980. Modelling of full wave acoustic logs. In: Paper Presented at the SPWLA 21st Annual Logging Symposium.
Dey, A.K., Stewart, R.R., 1997. Predicting density using vs and Gardner's relationship. CREWES Res. Rep. 9 (6), 1–9.
El-Alami, M., 1996. Habitat of oil in abu attiffel area, sirt basin, Libya. In: The Geology of the Sirt Basin, 2. Elsevier, Amsterdam, pp. 337–348.
El-Alami, M., Rahouma, S., Butt, A., 1989. Hydrocarbon habitat in the Sirte basin, northern Libya. Petrol. Res. J. 1, 19–30.
El-Bakush, H.S., Minas, A.H., Ghawar, B.M.B., 2010. Facha Member Reservoir, Fidaa Field– Sirte Basin. International Energy Foundation retrieved from.
El-Hawat, A.S., 1992. The Nubian Sandstone sequence in Sirte Basin, Libya: sedimentary facies and events. Geol. Arab World 1, 317–327.
El Hawat, A., Pawellek, T., 2004. A Field Guidebook to the Geology of Sirt Basin. RWE Dea North Africa, Libya.
Faraj, M.A.M., Knudsen, T.Š., Nytoft, H.P., Jovančićević, B., 2016. Organic geochemistry of crude oils from the Intisar oil field (East Sirte Basin, Libya). J. Petrol. Sci. Eng. 147, 605–616.
Frei, W., 1983. Sonic wave train analysis-a progress report. In: Paper Presented at the 8th European Formation Evaluation Symposium.
Gardner, G., Gardner, L., Gregory, A., 1974. Formation velocity and density—the diagnostic basics for stratigraphic traps. Geophysics 39 (6), 770–780.
Ghori, K., Mohammed, R., 1996. The Application of Petroleum Generation Modelling to the Eastern Sirt Basin, Libya. Geology of the Sirt Basin, 2. Elsevier, Amsterdam, pp. 529–540.
Gras, R., 1996. S. In: Tructural Style of the Southern Margin of the Messlah High. The Geology of the Sirt Basin, 3. Elsevier, Amsterdam, pp. 201–210.
Gumati, Y., Nairn, A., 1991. Tectonic subsidence of the Sirte basin, Libya. J. Petrol. Geol. 14 (1), 93–102.
Gumati, Y., Schamel, S., 1988. Thermal maturation history of the Sirte basin, Libya. J. Petrol. Geol. 11 (2), 205–218.
Hallett, D., Clark-Lowes, D., 2017. Petroleum Geology of Libya. Elsevier.
Krasovsky, S., 1981. Reflection of continental-type Crustal Dynamics in the Gravity Field. Navukova Dumka, Kiev.
Macgregor, D.S., Moody, R.T., 1998. Mesozoic and cenozoic petroleum systems of north africa. Geol. Soc. Lond. Spec. Publ. 132 (1), 201–216.
Mansour, A., Magairhy, I., 1996. Petroleum Geology and Stratigraphy of the southeastern Part of the Sirt Basin, Libya. The Geology of Sirt Basin, 2. Elsevier, Amsterdam, pp. 485–528.
Mavko, G., Mukerji, T., Dvorkin, J., 2009. The Rock Physics Handbook: Tools for Seismic Analysis of Porous media, second ed. ed. Cambridge university press, Cambridge, UK.
Montgomery, S., 1994. Sirte Basin, north-central Libya: Prospects for the Future, 11. Petroleum Information Corporation.
Musbah Abadi, A., 2002. Tectonics of the Sirt basin: Inferences from Tectonic Subsidence Analysis, Stress Inversion and Gravity Modeling, p. 187.
Nwozor, K., Onuorah, L.O., Onyekuru, S., Egbuachor, C., 2017. Calibration of Gardner coefficient for density–velocity relationships of tertiary sediments in Niger Delta Basin. J. Petrol. Exp. Prod. Technol. 7 (3), 627–635.
Pranter, M.J., Hurley, N.F., Davis, T.L., 2004. Anhydrite distribution within a shelf-margin carbonate reservoir: San Andres Formation, vacuum field, New Mexico, USA. Petrol. Geosci. 10 (1), 43–52.
Rafavich, F., Kendall, C.S.C., Todd, T., 1984. The relationship between acoustic properties and the petrographic character of carbonate rocks. Geophysics 49 (10), 1622–1636.
Roohi, M., 1996. Geological history and hydrocarbon migration pattern of the central Az Zahrah–Al Hufrah Platform. In: The Geology of Sirt Basin, 2. Elsevier, Amsterdam, pp. 435–454.
Rusk, D.C., 2001. AAPG Memoir 74, Chapter 22: Libya, Petroleum Potential of the Underexplored Basin Centers–A Twenty-First-Century Challenge, pp. 429–452.
Schlumberger, 2009. Log interpretation chart. In: Minerals, L.T. R.i.S. (Ed.), Appendix B). Sugar Land, Texas 77478. Schlumberger Wireline & Testing.
Serra, O., 2008. Well Logging Handbook, TECHNIP ed. Editions OPHRYS, Paris, France.